



**HAL**  
open science

## **Reliability and Accuracy of Time Resolved Contrast Enhanced Magnetic Resonance Angiography in Hypervascular Spinal Metastases prior Embolization**

Kevin Premat, Eimad Shotar, Robert Burns, Natalia Shor, Gauthier Eloy, Evelyne Cormier, Mehdi Drir, Laetitia Morardet, Stéphanie Lenck, Nader Sourour, et al.

► **To cite this version:**

Kevin Premat, Eimad Shotar, Robert Burns, Natalia Shor, Gauthier Eloy, et al.. Reliability and Accuracy of Time Resolved Contrast Enhanced Magnetic Resonance Angiography in Hypervascular Spinal Metastases prior Embolization. *European Radiology*, 2021, 10.1007/s00330-020-07654-3 . hal-03121093

**HAL Id: hal-03121093**

**<https://hal.sorbonne-universite.fr/hal-03121093v1>**

Submitted on 26 Jan 2021

**HAL** is a multi-disciplinary open access archive for the deposit and dissemination of scientific research documents, whether they are published or not. The documents may come from teaching and research institutions in France or abroad, or from public or private research centers.

L'archive ouverte pluridisciplinaire **HAL**, est destinée au dépôt et à la diffusion de documents scientifiques de niveau recherche, publiés ou non, émanant des établissements d'enseignement et de recherche français ou étrangers, des laboratoires publics ou privés.

# **Reliability and Accuracy of Time Resolved Contrast Enhanced Magnetic Resonance Angiography in Hypervascular Spinal Metastases prior Embolization**

Kévin Premat, MD<sup>1</sup>, Eimad Shotar, MD<sup>1</sup>, Robert Burns, MD<sup>1</sup>, Natalia Shor, MD<sup>1</sup>, Gauthier Eloy, MD<sup>2</sup>, Évelyne Cormier, MD<sup>1</sup>, Mehdi Drir, MD<sup>3</sup>, Laetitia Morardet, MD<sup>4</sup>, Stéphanie Lenck, MD<sup>1</sup>, Nader Sourour MD<sup>1</sup>, Jacques Chiras MD<sup>1</sup>, Didier Dormont, MD, PhD<sup>1</sup>, Raphaël Bonaccorsi, MD<sup>2</sup>, Frédéric Clarençon, MD, PhD<sup>1</sup>

<sup>1</sup> Sorbonne University, AP-HP, Pitié Salpêtrière - Charles Foix Hospital, Department of Neuroradiology, F75013, Paris, France

<sup>2</sup> Sorbonne University, AP-HP, Pitié Salpêtrière - Charles Foix Hospital, Department of Orthopaedic Surgery, F75013, Paris, France

<sup>3</sup> Sorbonne University, AP-HP, Pitié Salpêtrière - Charles Foix Hospital, Department of Anaesthesiology, F75013, Paris, France

<sup>4</sup> Sorbonne University, AP-HP, Pitié Salpêtrière - Charles Foix Hospital, Department of Oncology, F75013, Paris, France

Corresponding author: Kévin Premat, M.D.

Department of Neuroradiology. Pitié-Salpêtrière Hospital,

47-83 Boulevard de l'Hôpital, 75013 Paris, France

Mail : [kevin.premat@aphp.fr](mailto:kevin.premat@aphp.fr)

Phone: +33142163606

Fax: +33142183515

**Word count: 2811**

**Number of Figures: 4**

**Number of Tables: 3**

**Keywords:** Spine; Magnetic Resonance Angiography; Reproducibility of Results; Sensitivity and Specificity

## **ABSTRACT**

### **Objectives**

Preoperative embolization of Hypervascular Spinal Metastases (HSM) is efficient to reduce perioperative bleeding. However, intra-arterial digital subtraction angiography (IA-DSA) must confirm the hypervascular nature and rule out spinal cord arterial feeders. This study aimed to evaluate the reliability and accuracy of Time Resolved Contrast Enhanced Magnetic Resonance Angiography (TR-CE-MRA) in assessing HSM prior to embolization.

### **Methods**

All consecutive patients referred for preoperative embolization of an HSM were prospectively included. TR-CE-MRA sequences and selective IA-DSA were performed prior to embolization. Two readers independently reviewed imaging data to grade tumour vascularity (using a 3-grade and a dichotomized “yes vs no” scale) and identify the arterial supply of the spinal cord. Interobserver and intermodality agreements were estimated using kappa statistics.

### **Results**

Thirty patients included between 2016 and 2019 were assessed for 55 levels. Interobserver agreement was moderate ( $\kappa = 0.52$ ; 95% CI [0.09-0.81]) for TR-CE-MRA. Intermodality agreement between TR-CE-MRA and IA-DSA was good ( $\kappa = 0.74$ ; 95% CI [0.37-1.00]). TR-CE-MRA had a sensitivity of 97.9%, a specificity of 71.4%, a positive predictive value of 95.9%, a negative predictive value of 83.3% and an overall accuracy of 94.6%, for differentiating hypervascular from non-hypervascular SM. The arterial supply of the spine was assessable in 2/30 (6.7%) cases with no interobserver agreement ( $\kappa < 0$ ).

## **Conclusions**

TR-CE-MRA can reliably differentiate hypervascular from non-hypervascular SM and thereby avoid futile IA-DSAs. However, TR-CE-MRA was not able to evaluate the vascular supply of the spinal cord at the target levels, thus limiting its scope as a pretherapeutic assessment tool.

## **Key points**

1. TR-CE-MRA aids in distinguishing hypervascular from non-hypervascular spinal metastases.
2. TR-CE-MRA could avoid one quarter of patients referred for HSM embolization to undergo futile conventional angiography.
3. TR-CE-MRA's spatial resolution is insufficient to replace IA-DSA in the pretherapeutic assessment of the spinal cord vascular anatomy.

## **Keywords**

Spine; Magnetic Resonance Angiography; Reproducibility of Results; Sensitivity and Specificity

## **ABBREVIATIONS**

95% CI: 95% Confidence Interval

HSM: Hypervascular Spinal Metastasis (es)

IA-DSA: Intra Arterial Digital Subtraction Angiography

STARD: Standards for Reporting of Diagnostic Accuracy Studies

TAE: Transarterial Embolization

TRICKS: Time Resolved Imaging of Contrast Kinetics

TWIST: Time resolved angiography With Stochastic Trajectories

TR-CE-MRA: Time Resolved Contrast Enhanced Magnetic Resonance Angiography

## INTRODUCTION

The spine is a common site of bone metastases[1]. Spinal metastases can deteriorate the structural integrity of the vertebrae and potentially lead to pathological fractures with neurological symptoms. Spinal metastases can also expand into the surrounding soft tissues, and grow inside the epidural space eventually causing nerve or spinal cord compressions. At this point, urgent decompressive surgery is recommended to prevent debilitating neurological sequelae[2]. Hypervascular spinal metastases (HSM) are surgically challenging due to the high risk of perioperative hemorrhage that may hinder the extent of the resection and generate further complications[3]. Preoperative transarterial embolization (TAE) of HSMs can drastically reduce perioperative blood loss, thereby improving surgical resection [4, 5].

The hypervascular nature of a SM is suspected when dealing with histological type of primary malignancy that is frequently hypervascular, such as kidney, thyroid or hepatocellular neoplasms; or when tumour enhancement seems intense on postcontrast images [6]. Before proceeding to TAE, an intra-arterial digital subtraction angiography (IA-DSA) must confirm the hypervascular nature of the SM by showing a tumoral blush and rule out spinal cord arterial feeders at the target level or at an adjacent level. A non-invasive imaging technique that could replace IA-DSA could be of great use to avoid futile invasive examinations.

Time Resolved Contrast Enhanced Magnetic Resonance Angiography (TR-CE-MRA) is a DSA-like MRI sequence that provides dynamic visualization of the vascular system[7] at any given location. TR-CE-MRA is a widely available MRA sequence used for the evaluation of vascular anomalies throughout the entire body [8–11].

The objective of this study was to determine the diagnostic performance of TR-CE-MRA to assess the hypervascular nature of spinal metastases and detect a vascular supply of the spinal cord at the target levels.

## **MATERIALS AND METHODS**

The manuscript was prepared according to the 2015 Standards for Reporting of Diagnostic Accuracy Studies (STARD) guidelines[12].

### **Study design and participants**

This study is a monocenter prospective study that consecutively included patients with SM between 2016 and 2019 who met the following criteria:

1)  $\geq 18$  years old

2) SM of the cervical and/or thoracic and/or lumbar spine and/or the sacrum, defined as any osseous lesion of the spine that can be related to a histologically proven primary malignancy, either:

-By osseous biopsy

OR

- If the lesion appeared or grew on follow-up imaging (CT- and/or MRI-scans)

3) Interdisciplinary decision of surgical resection, required for at least one of the following reasons:

- Surgical decompression for spinal cord or nerve root compression

- Surgical stabilization

- Carcinologic surgery in mono or oligometastatic patients

4) Interdisciplinary decision of preoperative TAE, based on an estimation of the risk of major perioperative bleeding, for one of the following reasons:

- Primary malignancy that are frequently hypervascular (kidney, thyroid, melanoma or hepatocellular carcinoma).

OR

- SM with intense enhancement according to the assessment by the interdisciplinary team of available CT and/or MR images

Key exclusion criteria included:

1) Contraindication to MRI

2) Major contraindication to Gadolinium based- or iodinated contrast material

3) Major general comorbidity contraindicating surgery or embolization

4) Unavailability of TR-CE-MRA or IA-DSA images

5) Primary spinal tumours (benign or malignant)

Data collection was planned before the index and reference tests.

**Figure 1** illustrates the standardized imaging protocol used for all patients combining a full spine MRI with TR-CE-MRA sequences, followed by a spinal IA-DSA prior to embolization (during the same procedure), and lastly surgery within 48 hours after TAE.

## **Spine MRI protocol**

Spine MRIs were performed on 3T MRI systems (3T SIGNA HDX Advantage, General Electric, or 3T MAGNETOM Skyra, Siemens Healthineers). Two types of TR-CE-MRA were used depending on the MRI system; Time Resolved Imaging of Contrast Kinetics (TRICKS, General Electric)[7] or Time-resolved angiography With Stochastic Trajectories (TWIST, Siemens Healthineers)[13]. TR-CE-MRA sequences start with a non-contrast enhanced acquisition of the region of interest, followed by a series of images that show the transit of contrast material at approximately 1 or 2 frames per second, and finally stationary tissues are subtracted from the images. Contrast material injection protocol was standardized to optimize comparability [13]. All TR-CE-MRA sequences used a 3D-spoiled GRE sequence with thin slices and used a combination of ultra-short time of repetitions and time of echoes, low flip angles, parallel imaging and partial sampling of the k-space.

The main difference between the TRICKS and TWIST sequences is the way the k-space is partitioned and sampled. The TRICKS sequence divides the k-space into several concentric areas that are alternatively sampled while insisting on the central areas [7]; whereas the TWIST sequence divides the k-space into two concentric regions that are semi-randomly sampled [13].

## **IA-DSA and TAE procedures**

Interventions were performed under local anesthesia in most cases. General anesthesia was used for the TAE of cervical lesions. Intra-arterial CT angiography was performed similarly to a previously published study [14]. A femoral approach with a 5 French introducer was used to

place a 5 F Pigtail catheter (Cordis Corporation) at the origin of the descending aorta with a hybrid angiosuite (Miyabi Emotion 16, Siemens Healthineers), that combines a C-arm flat panel and a CT-scanner. The table was then translated toward the CT gantry to acquire an aortic CT-angiography. Guided by the aortic CT-angiography, spinal IA-DSA focused on the targeted level(s) was performed by selectively injecting iodine in the segmental arteries feeding the HSM, on both sides. Angiographic images were performed during breath holding of the patient. Radiculomedullary arteries including the arteries of Adamkiewicz or Von Haller were systematically searched for. Finally, the decision to undertake TAE was based on the hypervascular nature of the spinal metastasis and on the anatomy of the vascular supply of the spinal cord at the target level.

Only calibrated microparticles (300-500 $\mu$ m), pushable coils or gelatin sponges were used for the TAE of HSMs. As a safety rule, microparticles were forbidden at the same level or at an adjacent level of a radiculomedullary artery, in order to prevent inadvertent particle migration. Proximal occlusion (using coils and/or gelatin sponges) was also forbidden when a radiculomedullary feeder was seen on the same segmental branch.

### **Data collection and analysis**

All parameters used for defining tests results were defined prior to inclusions.

TR-CE-MRA and IA-DSA images were anonymized, analyzed independently over several sessions and reviewed independently in a random order by two senior neuroradiologists (7 and 15 years of experience) blinded to clinical data. The first reviewer performed a second

review of all TR-CE-MRA and IA-DSA images 6 months later in order to evaluate the intraobserver reliability.

Both reviewers independently assessed the following criteria:

- The overall quality of TR-CE-MRA examinations by using the following scale [8]: Grade 1: Poor image quality and/or major artifacts hindering interpretation. Grade 2: Moderate quality, still considered sufficient for interpretation. Grade 3: Good quality. Grade 1 sequences were interpreted and included in the analysis.

- The vascularity of SM on TR-CE-MRA sequences by using a simplified 3-point-scale version of a previously published classification [15]: Grade 1: Non-hypervascular (no significant enhancement). Grade 2: Mildly hypervascular (defined as a delayed and less intense enhancement compared to that of the aorta). Grade 3: Strongly hypervascular (defined as an enhancement similar to that of the aorta). The aorta was arbitrarily chosen as the reference for grading SM since it is the only vascular structure that can be reliably seen in all examinations. SM were then dichotomized into hypervascular (Grade 2 and 3) or non-hypervascular (Grade 1).

- The ability to identify the arterial feeders of the HSM as well as detect radiculomedullary branches feeding the anterior and posterolateral spinal arteries at the target level on TR-CE-MRA.

- The vascularity of SM on IA-DSA by using a simplified 3-point-scale version of a previously published classification [15]: Grade 1: Non-hypervascular (defined as a tumour stain < normal vertebral body). Grade 2: Mildly hypervascular (defined as a tumour stain similar to that of the normal vertebral body). Grade 3: Strongly hypervascular (defined as a tumour stain >

normal vertebral body). For this classification, the stain of the normal vertebral body was chosen as the reference. SM were then dichotomized into hypervascular (Grade 2 and 3) or non-hypervascular (Grade 1).

A consensual review of the discrepancies between the readers was used for the analysis.

**Figure 2** illustrates the main grading systems used in this study.

Patients' demographic data, pre- and postoperative clinical status, and procedure-related minor (local pain, puncture site hematoma) and major (stroke, new neurological deficit) complications were evaluated by reviewing patients' reports.

TR-CE-MRA was defined as the index test and was categorized as positive when the spinal metastasis was hypervascular (according to the dichotomized classification; i.e. Grade 2 and 3 SM on the 3-point-scale). IA-DSA was defined as the standard test and was categorized as positive when the SM was hypervascular according to the dichotomized classification.

### **Data analysis**

Interobserver and intraobserver agreements between TR-CE-MRA and IA-DSA images as well as intermodality agreement between TR-CE-MRA and IA-DSA images were assessed using Cohen's unweighted kappa statistics. Agreements were categorized as follows:  $\kappa \leq 0$ , no agreement;  $\kappa = 0.01-0.20$ , poor;  $\kappa = 0.21-0.40$ , fair;  $\kappa = 0.41-0.60$ , moderate;  $0.61-0.80$ , good;  $0.81-0.90$ , very good and  $\kappa > 0.90$ : almost perfect. Diagnostic performance was estimated by calculating the sensitivity, the specificity, the predictive values and the accuracy. All analyses were performed with MedCalc Version 19.2.0 (MedCalc Software Ltd).

## **Ethical Statement**

The protocol of this study was approved by the local institutional review board (Comité de Protection des Personnes d'Ile-de-France n°HH\_16\_04\_20).

Additional details regarding the study methodology are available in **Supplemental Material**.

## RESULTS

Thirty patients (mean age: 65.5 ±13.5 years; range: 36-81) were included and assessed for 55 affected levels. Of note, one patient included had two preoperative TAEs and two TR-CE-MRA 12 months apart, at two different levels and was included twice. **Table 1.** details patients' baseline characteristics. TAE was performed for twenty out of thirty patients (66.7%). Reasons for challenging TAE's indication were the absence of significant tumoral blush (8/30 [26.7%]) or proof of radiculomedullary branch at the target level (5/30 [16.7%]). No minor or major complications occurred after performing the index or standard test. One major complication (3.3%) occurred during TAE, which consisted of the deterioration of a lower limb deficit immediately after the injection of 3mL of polyvinyl alcohol particles, supposedly consecutive to ischemic injuries. There were no signs of spinal ischemia on the MRI performed immediately after the procedure. The patient underwent surgery as planned and his deficit improved, therefore no follow-up MRI was performed. **Figure 3.** summarizes the flow of patients throughout the study. The diagnosis of SM required a biopsy in 4/30 (13.3%). For the remaining 27 patients, it was strongly suspected based on the progression on follow-up imaging. The final diagnosis of SM was confirmed in all cases after histologic analysis of surgical samples.

### Agreement study

TR-CE-MRA and IA-DSA were performed for all patients. The overall quality of TR-CE-MRA was deemed sufficient for interpretation in 27/30 (90%) of cases, irrespectively of the type of sequence (10/11 [90.9%] of TWIST sequences versus 17/19 [89.5%] of TRICKS [ $p=0.89$ ]) or the acquisition plane (16/17 [94.1%] in sagittal plane versus 11/13 [84.6%] in coronal plane [ $p=0.39$ ]). Interobserver agreement was fair for grading hypervascularity on a 3-point-scale ( $\kappa$

= 0.21; 95% CI [0.01-0.43]) and moderate when using the dichotomized version on TR-CE-MRA ( $\kappa = 0.52$ ; 95% CI [0.09-0.81]). On IA-DSA, interobserver agreement was good for judging hypervascularity on the 3-point-scale ( $\kappa = 0.62$ ; 95% CI [0.39-0.80]) and very good for the dichotomized version ( $\kappa = 0.85$ ; 95% CI [0.56-1.00]). Intraobserver agreements were fair ( $\kappa = 0.40$ ; 95% CI [0.19-0.61]) and moderate ( $\kappa = 0.59$ ; 95% CI [0.39-0.90]) for the 3-grade and dichotomized scales for TR-CE-MRA. Intraobserver agreement was good ( $\kappa = 0.74$ ; 95% CI [0.45-0.1]) for the 3-grade scale and very good ( $\kappa = 0.85$ ; 95% CI [0.55-0.1]) for the dichotomized version for IA-DSA. Intermodality agreement was moderate for assessing tumour vascularity on the 3-grade-scale ( $\kappa = 0.43$ ; 95% CI [0.17-0.64]) and good when using the dichotomized classification ( $\kappa = 0.74$ ; 95% CI [0.37-1.00]). **Table 2** summarizes TR-CE-MRA and IA-DSA findings and **Table 3** summarizes inter-/intraobserver and intermodality agreements for tumour vascularity assessment.

On TR-CE-MRA, radiculomedullary branches feeding the spinal cord arteries were consensually seen in 2/30 cases (6.7%) with no agreement between observers ( $\kappa = -0.3$ ; 95% CI [-0.9-0]) and arterial feeders to the metastases could be seen in 27/55 cases (49.1%) with moderate interobserver reliability ( $\kappa = 0.42$ ; 95% CI [0.15-0.64]).

### **Diagnostic performance of TR-CE-MRA**

Detailed results are summarized in the STARD flow diagram in **Figure 4**.

When confronted to IA-DSA as the gold standard, TR-CE-MRA showed a sensitivity of 97.9% (95% CI [88.9-99.9]), a specificity of 71.4% (95% CI [29.0-96.3]), a positive predictive value of 95.9% (95% CI [87.9-98.7]), a negative predictive value of 83.3% (95% CI [40.5-97.4]) and an

overall accuracy of 94.6% (95% CI [84.9-98.9]), for differentiating hypervascular from non-hypervascular SM.

## DISCUSSION

This study confirms that the histological type of the primary malignancy and the subjective appraisal of the tumoral enhancement on conventional MR sequences cannot reliably determine whether a SM is hypervascular. In this series, 26.7% of supposedly HSM were non-hypervascular on IA-DSA and were recused from TAE.

The results showed that both manufacturers' MRI machines could consistently produce TR-CE-MRA images of the spine with satisfying image quality. Even though the inter- and intraobserver reliability to evaluate tumour vascularity was better for IA-DSA, TR-CE-MRA was still reproducible between trained radiologists and correlated to IA-DSA. However, interobserver and intermodality agreements were only satisfactory when using a dichotomized version. Stratification of the tumour's vascularity, even when using a simple 3-grade-scale was not reproducible among observers on TR-CE-MRA. Intraobserver agreement study also supported this finding. Negative predictive value and specificity for vascularity assessment, which are the most pertinent indicators, were good. The main limit of the technique is it could not consistently depict the radiculomedullary feeders to the spinal cord.

Preoperative TAE has been previously reported as a safe and effective technique to prevent massive perioperative bleeding in HSM[16] and is now performed in numerous institutions. Other studies have shown that preoperative TAE failed to reduce perioperative blood losses in non-hypervascular SM [17]. Debates over its efficacy in non-hypervascular SM are still ongoing but, for now, they are not a clear indication for preoperative TAE because of an unfavorable risk/benefit balance. TAE is an invasive procedure that entails a risk of spinal cord ischemic injuries that justifies an extensive assessment of the spinal cord vascular supply.

Therefore, TAE is contraindicated if a radiculomedullary branch arises at the target level or at an immediately adjacent level [18].

IA-DSA is the technique that provides the highest spatial resolution and is the current gold standard for assessing a spinal tumour's vascularity but is also associated with complications, such as embolism and puncture-site bleeding[19].

Several non-invasive imaging techniques have been studied in this indication with promising results. Dual-energy CTA which allows acquisition of several time phases after intravenous injection of iodinated contrast material can reliably assess the vascularity of spine metastases both qualitatively and quantitatively [15]. Dynamic contrast enhanced MR perfusion sequences have also been used, and seem capable of distinguishing HSM from non-HSM through quantitative measurements[20]. The main issues with these techniques are that the first requires high radiation exposure and only allows exploration of a limited volume; the latter is a more advanced technique, not widely available, and that requires an additional postprocessing workload. As such, both techniques may arguably be of limited use in clinical routine.

Conversely, TR-CE-MRA sequences of the spine are routinely performed in the exploration of spinal or paraspinal arteriovenous shunts [9, 21]; and are thus widely available in almost all MR systems. They have already been proven to be reliable for evaluating the tumour stain of hypervascular head and neck tumours in comparison to the gold standard IA-DSA[8]. However, similarly to previous studies, we found that TR-CE-MRA was not capable of adequately assessing the spinal cord vascular anatomy and therefore cannot replace IA-DSA for preoperative assessment.

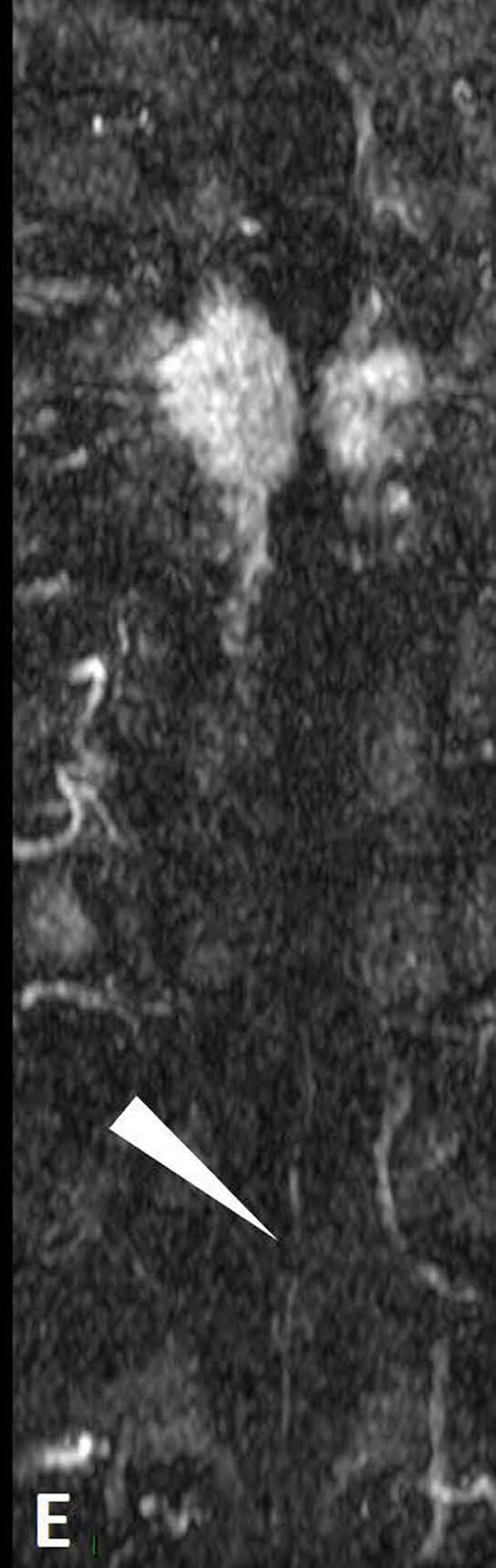
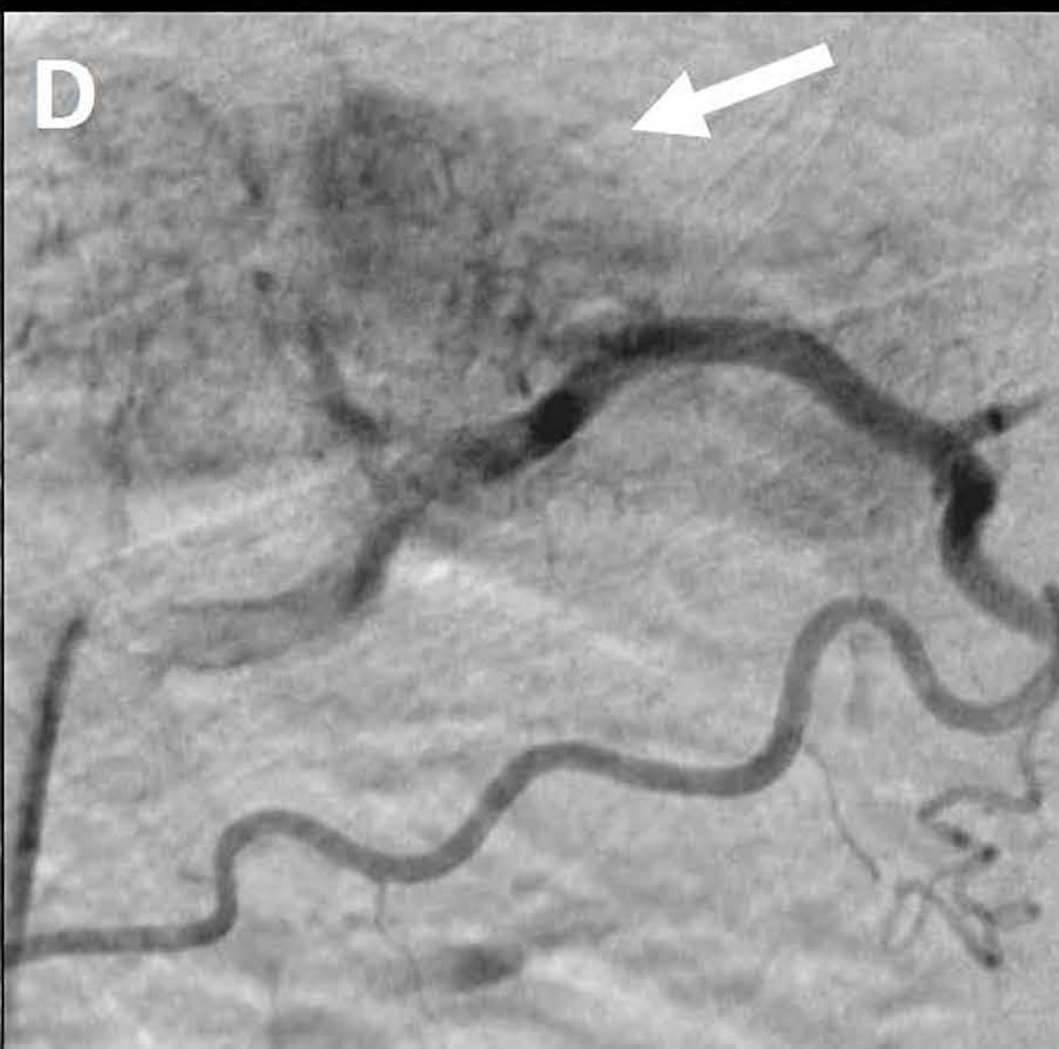
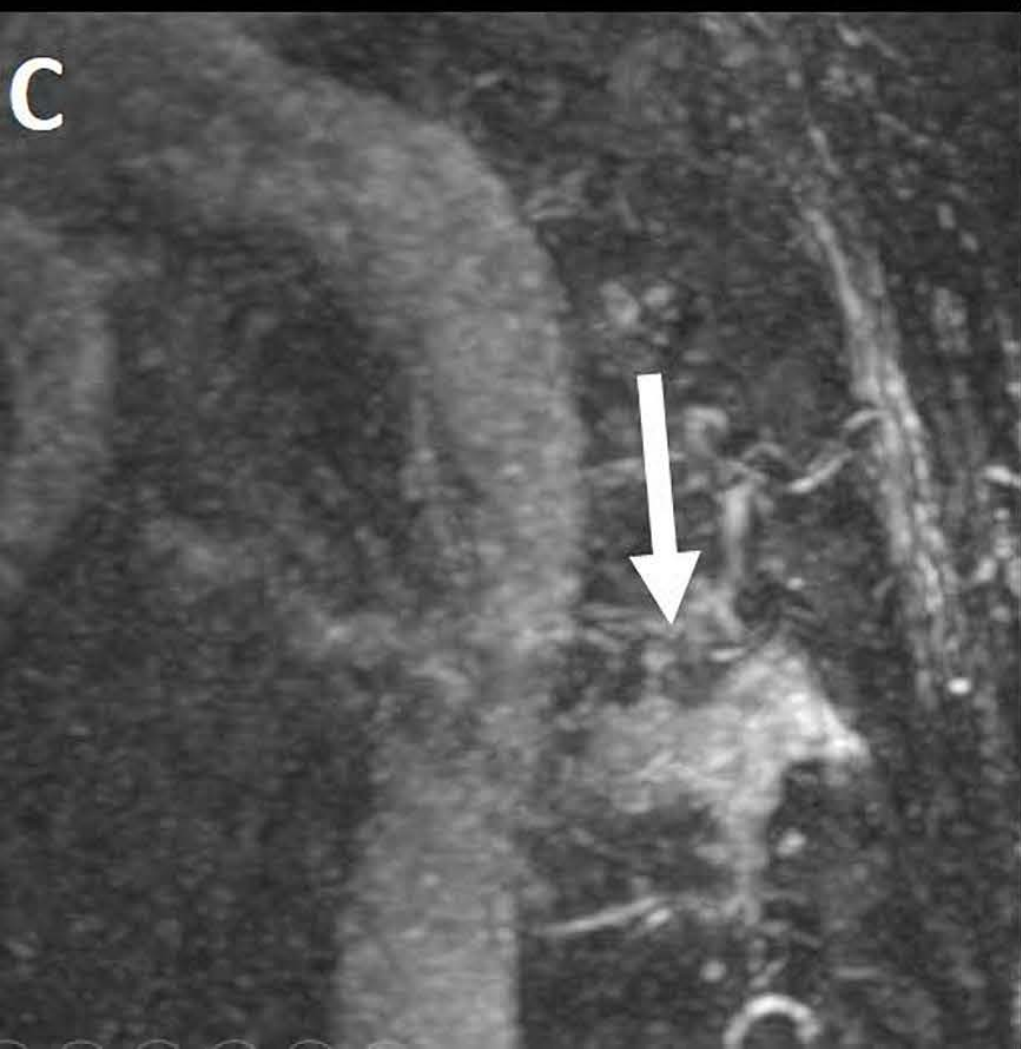
This study has limitations. First the monocentric fashion of data collection as well as the low number of patients limits the extrinsic value of the study. Second, we included some patients with SMs that were considered strongly enhanced on non-invasive imaging. This subjective inclusion criterion may have heterogenized the study population. Finally, the low number of negative patients (i.e.: non-hypervascular SM) is a bias to accurately estimate the specificity and the negative predictive value, which are the most critical indicators to consider in these cases to safely rule out HSM. However, this is the first study to date to emphasize on this widely available MRA sequence in HSM.

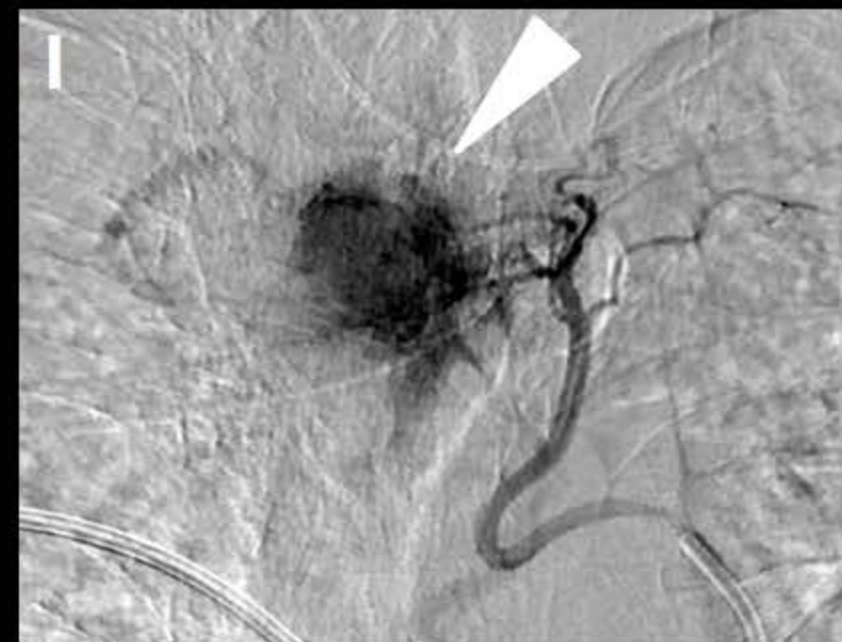
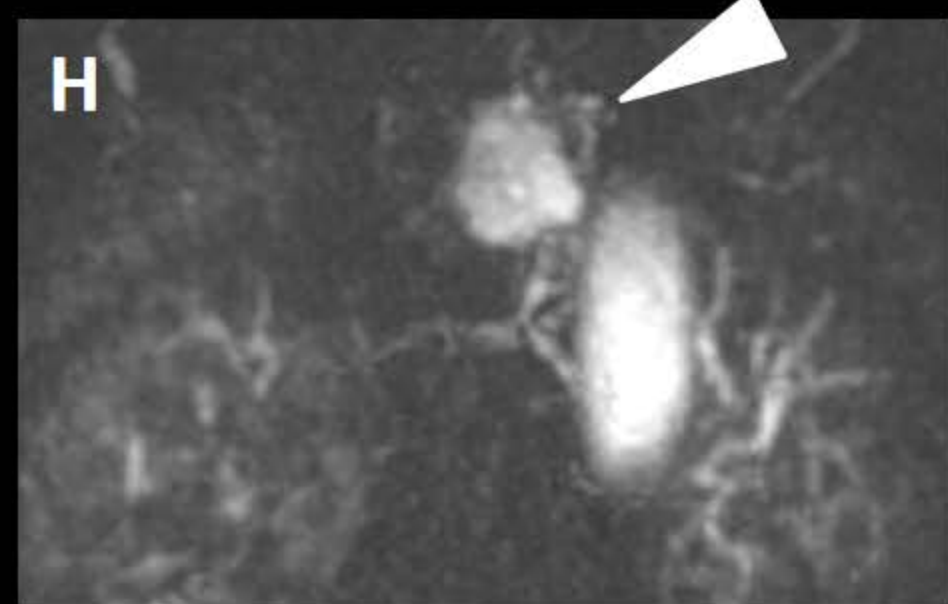
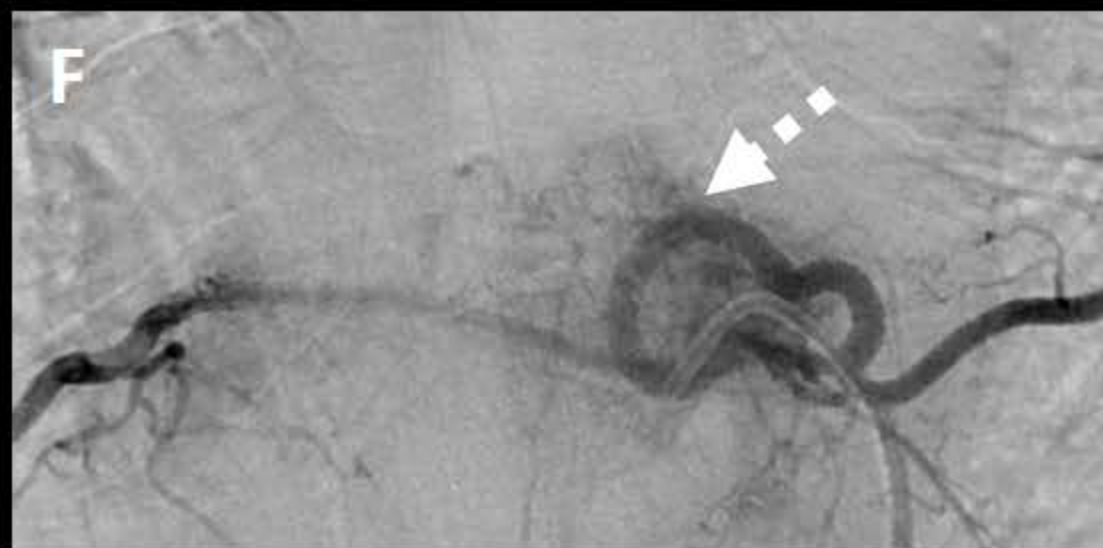
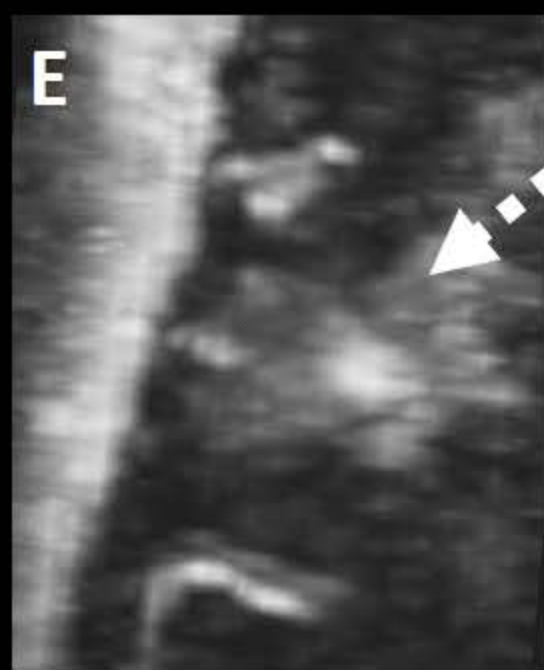
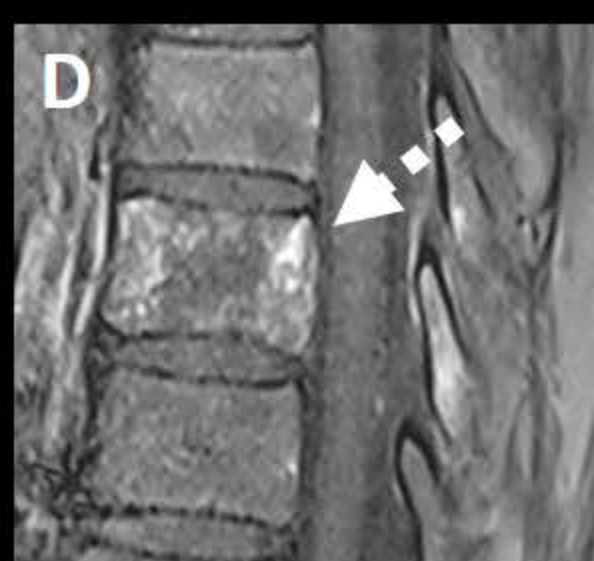
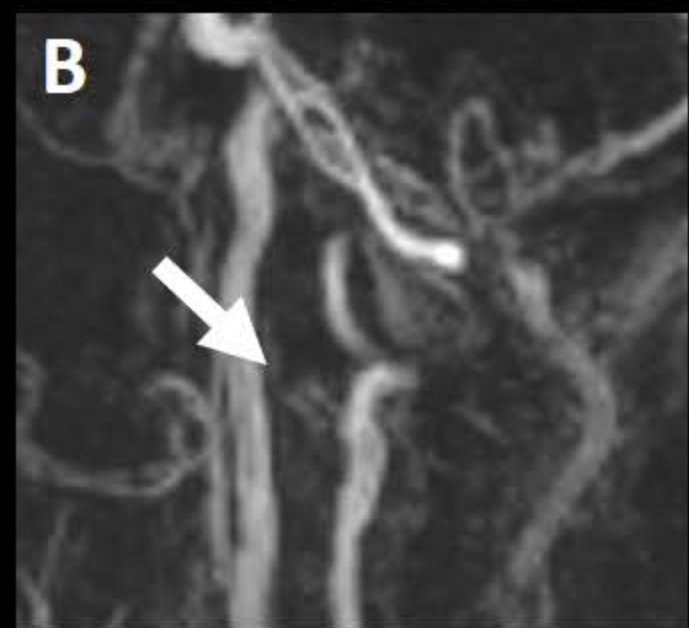
In conclusion, this study confirms that a significant proportion of HSM referred for preoperative TAE are recused after IA-DSA for two main reasons: the non-hypervascular nature of the SM or proof of a contiguous arterial supply to the spinal cord. TR-CE-MRA seems reliable and accurate for assessing the vascularity of SM, however, its spatial resolution did not allow proper evaluation of the arterial supply of the spinal cord in the vicinity of the target level.

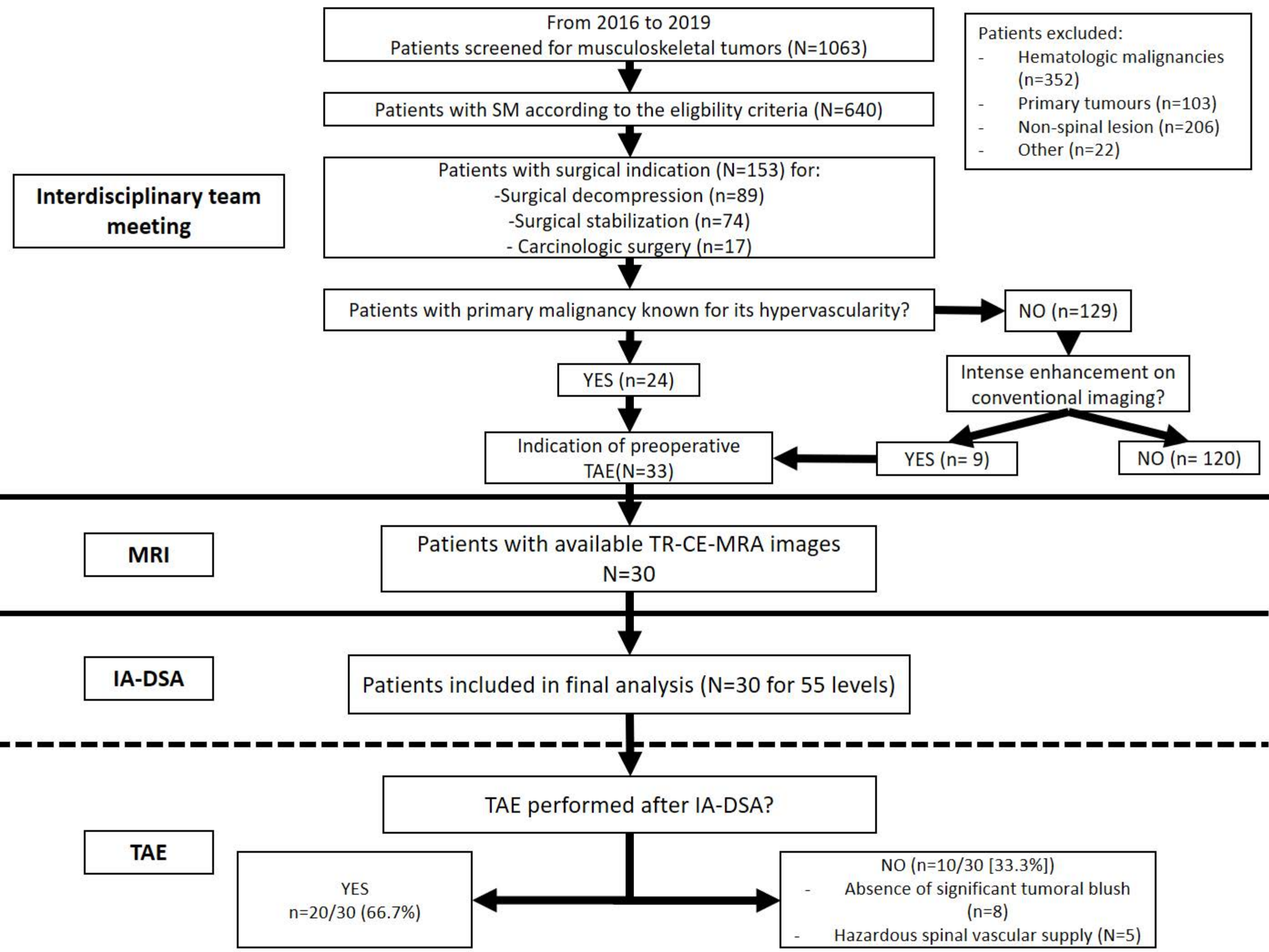
## REFERENCES

1. Li S, Peng Y, Weinhandl ED, et al (2012) Estimated number of prevalent cases of metastatic bone disease in the US adult population. *Clin Epidemiol* 4:87–93. <https://doi.org/10.2147/CLEP.S28339>
2. Spratt DE, Beeler WH, de Moraes FY, et al (2017) An integrated multidisciplinary algorithm for the management of spinal metastases: an International Spine Oncology Consortium report. *Lancet Oncol* 18:e720–e730. [https://doi.org/10.1016/S1470-2045\(17\)30612-5](https://doi.org/10.1016/S1470-2045(17)30612-5)
3. Tang B, Ji T, Tang X, et al (2015) Risk factors for major complications in surgery for hypervascular spinal tumors: an analysis of 120 cases with adjuvant preoperative embolization. *Eur Spine J Off Publ Eur Spine Soc Eur Spinal Deform Soc Eur Sect Cerv Spine Res Soc* 24:2201–2208. <https://doi.org/10.1007/s00586-015-4122-8>
4. Guzman R, Dubach-Schwizer S, Heini P, et al (2005) Preoperative transarterial embolization of vertebral metastases. *Eur Spine J Off Publ Eur Spine Soc Eur Spinal Deform Soc Eur Sect Cerv Spine Res Soc* 14:263–268. <https://doi.org/10.1007/s00586-004-0757-6>
5. Griessenauer CJ, Salem M, Hendrix P, et al (2016) Preoperative Embolization of Spinal Tumors: A Systematic Review and Meta-Analysis. *World Neurosurg* 87:362–371. <https://doi.org/10.1016/j.wneu.2015.11.064>
6. Khadem NR, Karimi S, Peck KK, et al (2012) Characterizing hypervascular and hypovascular metastases and normal bone marrow of the spine using dynamic contrast-enhanced MR imaging. *AJNR Am J Neuroradiol* 33:2178–2185. <https://doi.org/10.3174/ajnr.A3104>
7. Korosec FR, Frayne R, Grist TM, Mistretta CA (1996) Time-resolved contrast-enhanced 3D MR angiography. *Magn Reson Med* 36:345–351. <https://doi.org/10.1002/mrm.1910360304>
8. Nishimura S, Hirai T, Shigematsu Y, et al (2012) Evaluation of brain and head and neck tumors with 4D contrast-enhanced MR angiography at 3T. *AJNR Am J Neuroradiol* 33:445–448. <https://doi.org/10.3174/ajnr.A2819>
9. Condette-Auliac S, Boulin A, Roccatagliata L, et al (2014) MRI and MRA of spinal cord arteriovenous shunts. *J Magn Reson Imaging* 40:1253–1266. <https://doi.org/10.1002/jmri.24591>
10. Hammer S, Uller W, Manger F, et al (2017) Time-resolved magnetic resonance angiography (MRA) at 3.0 Tesla for evaluation of hemodynamic characteristics of vascular malformations: description of distinct subgroups. *Eur Radiol* 27:296–305. <https://doi.org/10.1007/s00330-016-4270-1>

11. Dautry R, Edjlali M, Roca P, et al (2015) Interest of HYPR flow dynamic MRA for characterization of cerebral arteriovenous malformations: comparison with TRICKS MRA and catheter DSA. *Eur Radiol* 25:3230–3237. <https://doi.org/10.1007/s00330-015-3745-9>
12. Cohen JF, Korevaar DA, Altman DG, et al (2016) STARD 2015 guidelines for reporting diagnostic accuracy studies: explanation and elaboration. *BMJ Open* 6:e012799. <https://doi.org/10.1136/bmjopen-2016-012799>
13. Hennig J, Scheffler K, Laubenberger J, Strecker R (1997) Time-resolved projection angiography after bolus injection of contrast agent. *Magn Reson Med* 37:341–345. <https://doi.org/10.1002/mrm.1910370306>
14. Clarençon F, Di Maria F, Sourour N-A, et al (2016) Evaluation of intra-aortic CT angiography performances for the visualisation of spinal vascular malformations' angioarchitecture. *Eur Radiol* 26:3336–3344. <https://doi.org/10.1007/s00330-015-4204-3>
15. Huang Y-C, Tsuang F-Y, Lee C-W, et al (2019) Assessing Vascularity of Osseous Spinal Metastases with Dual-Energy CT-DSA: A Pilot Study Compared with Catheter Angiography. *AJNR Am J Neuroradiol* 40:920–925. <https://doi.org/10.3174/ajnr.A6023>
16. Luksanaprukpa P, Buchowski JM, Tongchai S, et al (2018) Systematic review and meta-analysis of effectiveness of preoperative embolization in surgery for metastatic spine disease. *J Neurointerventional Surg* 10:596–601. <https://doi.org/10.1136/neurintsurg-2017-013350>
17. Yoo S-L, Kim Y-H, Park H-Y, et al (2019) Clinical Significance of Preoperative Embolization for Non-Hypervascular Metastatic Spine Tumors. *J Korean Neurosurg Soc* 62:106–113. <https://doi.org/10.3340/jkns.2018.0073>
18. Nair S, Gobin YP, Leng LZ, et al (2013) Preoperative Embolization of Hypervascular Thoracic, Lumbar, and Sacral Spinal Column Tumors: Technique and Outcomes from a Single Center. *Interv Neuroradiol* 19:377–385
19. Forbes G, Nichols DA, Jack CR, et al (1988) Complications of spinal cord arteriography: prospective assessment of risk for diagnostic procedures. *Radiology* 169:479–484. <https://doi.org/10.1148/radiology.169.2.3174997>
20. Saha A, Peck KK, Lis E, et al (2014) Magnetic resonance perfusion characteristics of hypervascular renal and hypovascular prostate spinal metastases: clinical utilities and implications. *Spine* 39:E1433-1440. <https://doi.org/10.1097/BRS.0000000000000570>
21. Vargas MI, Nguyen D, Viallon M, et al (2010) Dynamic MR angiography (MRA) of spinal vascular diseases at 3T. *Eur Radiol* 20:2491–2495. <https://doi.org/10.1007/s00330-010-1815-6>







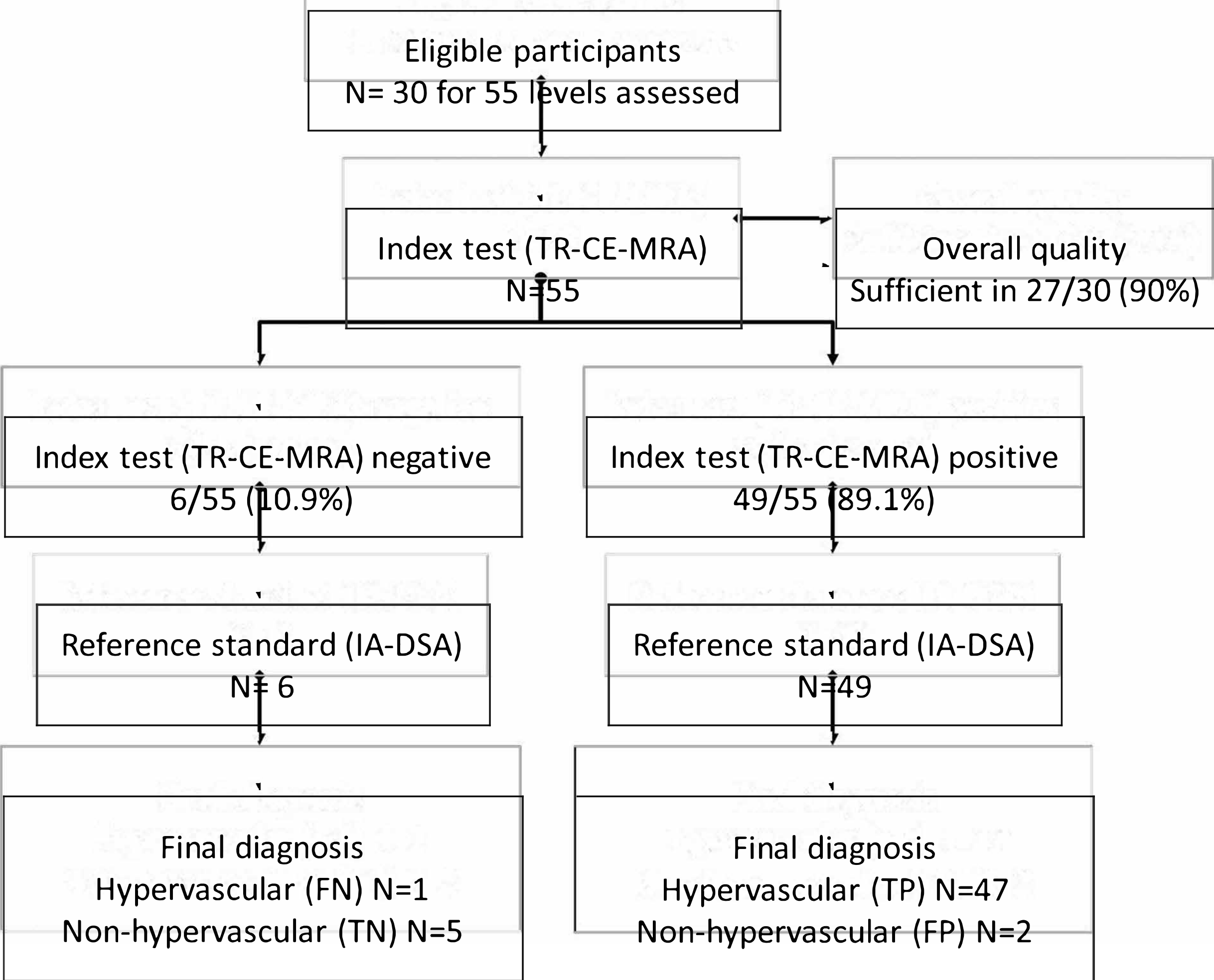


## FIGURE LEGENDS

### Figure 1. Illustrative case of the study findings

Middle-aged patient with a vertebral (T8) metastasis of a renal cell carcinoma. **A. and B.** Spine MRI; respectively sagittal unenhanced T2 Fast Spin Echo and contrast enhanced T1 Spin Echo sequences showed a vertebral mass of T8 with posterior wall involvement and a compressive epidural extension (white arrow). After multidisciplinary meeting, a decision to undertake surgery with preoperative TAE was retained. **C.** Late arterial phase TR-CE-MRA sequence (TRICKS) in the sagittal plane; showed a strongly hypervascular (Grade 3) spinal metastasis (white arrow), confirmed by IA-DSA (D; left anterior oblique view). Even though the anterior spinal artery could be seen on TR-CE-MRA (E; white arrowhead), its radiculomedullary contributor could not be viewed.

**Figure 2.** Illustration of the various grading scales used for the classification of tumour vascularity on TR-CE-MRA and IA-DSA.

**A:** Spine MRI, Sagittal T2 Fast Spin Echo sequence: Young adult patient with a vertebral metastasis (C3) of a cholangiocarcinoma (White arrow). **B:** Sagittal TR-CE-MRA sequence showing no significant tumoral stain (White arrow), confirmed by IA-DSA (lateral projection) **(C).** **D, E and F:** Respectively, sagittal FAT-SAT T1 contrast enhanced sequence, sagittal TR-CE-MRA sequence (late arterial phase) and anteroposterior IA-DSA projection of a mildly hypervascular metastasis of T3 (White dotted arrows) secondary to renal cell carcinoma in an elderly patient. **G, H, I:** Respectively, sagittal Short TI Inversion Recovery (STIR) sequence, coronal TR-CE-MRA sequence (early arterial phase) and anteroposterior IA-DSA projection of

a strongly hypervascular metastasis of the posterior arch of T3 (White arrowheads) in an elderly patient.

**Figure 3.** Flow diagram of the study

SM: Spinal Metastasis (es); TAE: Trans Arterial Embolization; TR-CE-MRA: Time Resolved Contrast Enhanced Magnetic Resonance Angiography; IA-DSA: Intra Arterial Digital Subtracted Angiography

**Figure 4.** Standards for Reporting of Diagnostic Accuracy Studies flow diagram of participants throughout the study

TR-CE-MRA: Time Resolved Contrast Enhanced Magnetic Resonance Imaging; IA-DSA: intra-arterial digital subtraction angiography; FN: False Negative; TN: True Negative; TP: True Positive; FP: False Positive

## TABLES LEGENDS

**Table 1.** Baseline characteristics of the population

† n/tot. Number/total; \* i.e, fixation and/or decompressive surgery; ® 4D Contrast Enhanced Magnetic Resonance Angiography; <sup>1</sup> Time-resolved imaging of contrast kinetics; <sup>2</sup> Time-resolved angiography With Stochastic Trajectories

**Table 2.** Summary of TR-CE-MRA and IA-DSA findings

TR-CE-MRA: Time Resolved Contrast Enhanced Magnetic Resonance Angiography; IA-DSA: Intra-Arterial Digital Subtraction Angiography; N/tot. Number/total; NE: Not Evaluated

**Table 3.** Inter-/intraobserver and intermodality agreements for tumour vascularity assessment

TR-CE-MRA: Time Resolved Contrast Enhanced Magnetic Resonance Angiography; IA-DSA: Intra-Arterial Digital Subtraction Angiography

## SUPPLEMENTAL MATERIAL

### ADDITIONAL MATERIALS AND METHODS

#### Spine MRI protocol

Spine MRIs were performed on 3T MRI systems (3T SIGNA HDX Advantage, General Electric; or 3T MAGNETOM Skyra, Siemens Healthineers). The standard protocol included full spine sagittal T2 fast spin echo and T1 spin echo sequences, optional axial T2 fast spin echo slices and mandatory post contrast T1 spin echo sagittal and axial slices. TR-CE-MRA acquisitions were performed on the target level, either in sagittal or coronal planes.

For the TRICKS sequences, the acquisition parameters were as follows: Field of view: 300mm; Slice thickness: 2mm; Time of repetition: 3.9ms; Time of echo: 1.5ms; Flip angle: 18°; acceleration factor: 2; number of phases: 30.

For the TWIST sequence, the acquisition parameters were as follows: Field of view: 230mm; Slice thickness: 1mm; voxel size: 0.9x0.9x1mm; Time of repetition: 2.21ms; Time of echo: 0.96ms; Flip angle: 18°; acceleration factor: 2; number of phases: 40.

The standard protocol of contrast material injection was performed using automated intravenous injections of 0.2 mL of gadoteric acid (Dotarem, Guerbet) per kilogram of body weight (flow rate: 1.5 mL/s), flushed by 20mL of saline.

#### IA-DSA and TAE procedures

Interventions at the cervical level were all performed in a biplane angiosuite under general anesthesia. For thoracic, lumbar and sacral levels, the procedures were performed in a hybrid angiographic suite (Miyabi Emotion 16, Siemens Healthineers) combining a C-arm flat panel and a CT-scan (Somatom Emotion 16 rows, Siemens Healthineers), under local anesthesia.

#### Data analysis

Interobserver agreement between TR-CE-MRA and IA-DSA images as well as intermodality agreement between consensus readings of TR-CE-MRA and IA-DSA images were assessed using Cohen's unweighted kappa statistics. Analyses were performed with 95% bias-corrected confidence intervals obtained by 1000 bootstrap resampling. Kappa coefficients values were expressed with their 95% confidence intervals (95% CI). Comparisons of proportions were performed using a  $\chi^2$  test, with a significance threshold set at 0.05. Diagnostic performances were estimated by calculating the sensitivity, the specificity, the predictive values and the accuracy. Diagnostic performances parameters were expressed in percentages surrounded by their 95% CI.

**Table 1.** Baseline characteristics of the population

Parameter	n/tot.† (%)
<b>Sex</b>	11/30 Females (36.7), 19/30 Males (63.3)
<b>Levels assessed (n=55)</b>	
- Cervical	8/55 (14.5)
- Thoracic	31/55 (56.4)
- Lumbar	15/55 (27.3)
- Sacral	1/55 (1.8)
- Single level	14/30 (46.7)
- Multiple levels	16/30 (53.3)
<b>Primary malignancy</b>	
- Kidney	12/30 (40)
- Thyroid	7/30 (23.3)
- Hepatocellular carcinoma	5/30 (16.7)
- Other (lung, breast, prostate, cholangiocarcinoma, bladder and unknown)	6/30 (20)
<b>Interventions close the target level prior inclusion</b>	
- Surgery*	5/30 (16.7)
- Percutaneous vertebroplasty	6/30 (20)
<b>Sequence used for 4D-CE-MRA®</b>	
- TRICKS‡	11/30 (37.9)
- TWIST§	19/30 (63.3)

† n/tot. Number/total; \* i.e, fixation and/or decompressive surgery; ® 4D Contrast Enhanced Magnetic Resonance Angiography; ‡ Time-resolved imaging of contrast kinetics; § Time-resolved angiography With Stochastic Trajectories

**Table 2.** Summary of TR-CE-MRA and IA-DSA findings

	TR-CE-MRA		IA-DSA	
	N/tot. (%)		N/tot. (%)	
Investigators	#1	#2	#1	#2
Tumor vascularity				
-Grade 1	5/55 (9.1)	9/55 (16.4)	8/55 (14.5)	8/55 (14.5)
-Grade 2	19/55 (34.5)	22/55 (40)	14/55 (25.5)	17/55 (30.9)
-Grade 3	31/55 (56.4)	24/55 (43.4)	33/55 (60)	30/55 (54.6)
Tumor vascularity dichotomized n(%)				
-Hypervascular	50/55 (90.9)	46/55 (83.6)	47/55 (85.5)	47/55 (85.5)
-Non-hypervascular	5/55 (9.1)	9/55 (16.4)	8/55 (14.5)	8/55 (14.5)
Overall image quality				
n (%)				
-Grade 1 (Poor)	5/30 (16.7)	2/30 (6.7%)	NE	NE
-Grade 2 (Moderate)	16/30 (53.3)	14/30 (46.7)		
-Grade 3 (Good)	9/30 (30)	14/30 (46.7)		

TR-CE-MRA: Time Resolved Contrast Enhanced Magnetic Resonance Angiography; IA-DSA: Intra-Arterial Digital Subtraction Angiography; N/tot. Number/total; NE: Not Evaluated

**Table 3.** Inter-/intra-observer and intermodality agreements for tumour vascularity assessment

	Interobserver agreement	Intraobserver agreement	Intermodality (TR-CE-MRA with IA-DSA) agreement
Tumour vascularity (3-grade scale)	0.21 [0.01-0.43]	0.40 [0.19-0.61]	0.43 [0.17-0.64]
-TR-CE-MRA	0.62 [0.39-0.80]	0.59 [0.39-0.90]	
- IA-DSA			
Tumour vascularity (dichotomized)	0.52 [0.09-0.81]	0.74 [0.45-1]	0.74 [0.37-1.00]
-TR-CE-MRA	0.85 [0.56-1.00]	0.85 [0.55-1]	
- IA-DSA			
Visible radiculomedullary branch on TR-CE-MRA	-0.3 [-0.9-0.00]		
Visible arterial feeder on TR-CE-MRA	0.42 [0.15-0.64]		

TR-CE-MRA: Time Resolved Contrast Enhanced Magnetic Resonance Angiography; IA-DSA: Intra-Arterial Digital Subtraction Angiography